PERGAMON

Journal of Structural Geology 25 (2003) 503–513

JOURNAL OF STRUCTURAL GEOLOGY

www.elsevier.com/locate/jstrugeo

Formation of normal faults along the axial zone of the Ethiopian Rift

V. Acocella[a,*], T. Korme[b], F. Salvini[a]

[a]*Dip. Scienze Geologiche Roma TRE. Largo S.L. Murialdo, 1, 00146 Roma, Italy*
[b]*Dept. of Geology and Geophysics, Addis Ababa University, PO Box 1176, Addis Ababa, Ethiopia*

Received 30 July 2001; accepted 15 March 2002

Abstract

The axial zone of the Ethiopian Rift is made up of Quaternary extensional fractures and normal faults. Field analysis was performed to study the mechanism of development of the normal faults. The collected data show that the normal faults (1) are subvertical at surface, (2) have dilation proportional to the throw, and (3) end laterally as extension fractures, that is, tension fractures which gradually decrease in dilation. The minimum measured opening of normal faults is 2 m and the maximum measured dilation of the extension fractures is 4 m. The minimum measured length of normal faults is 800 m and the maximum measured length of the extension fractures is 400 m. The collected data suggest that the normal faults nucleate from wider extension fractures in the axial zone. When the extension fractures reach critical dimensions (length = ~800 m and dilation = 2–4 m, corresponding to a predicted depth of ~700 m), the shear rupture behavior controls the further propagation of the fractures at depth. This mechanism has close similarities with models previously proposed for fault formation along the oceanic ridge of Iceland. This suggests common rifting processes along diverging plates, independently from the oceanic or continental nature of the lithosphere.

Keywords: Ethiopian Rift; Normal faults; Extension fractures

1. Introduction

Normal faults are commonly well developed features in rift zones. Among these, active narrow rift zones (sensu Buck, 1991) are characterized by a focused area of extension and offer the opportunity to observe, within a limited area, normal faults at different stages of evolution. Narrow rifts are found in both continental and oceanic domains; among the best-known examples are the East African Rift System and the oceanic ridge of Iceland.

These rift zones are made of several interacting extensional segments (Bonatti, 1985; Ebinger et al., 1987; Ebinger, 1989; Gudmundsson, 1992, 1995; Nelson et al., 1992; Hayward and Ebinger, 1996). At the early stages, these usually consist of half graben-like structures, interacting and evolving towards symmetry and turning into graben-like structures at later stages (Ebinger et al., 1984; Bosworth, 1985; Gudmundsson, 1987a,b; Rosendahl, 1987; Morley, 1988; Woldegabriel et al., 1990; Scholz and Contreras, 1998; Kazmin and Byakov, 2000). Regardless of these asymmetries, a narrow rift shows an inner, younger and active zone of extension, characterized by subparallel extension fractures and normal faults, whose vertical displacements increase from the axial zone towards the mature rift margins (Mohr, 1968; Needham et al., 1976; Tamsett, 1986; Martinez and Cochran, 1988; Forslund and Gudmundsson, 1991, 1992; Angelier et al., 1997). It is commonly accepted that subparallel extension fractures and normal faults form contemporaneously and independently under the same stress conditions in the axial part of a rift (Mohr, 1968; Gibson, 1969; Pollard et al., 1983; Tamsett, 1986).

Several works have addressed the details of formation and development of normal faults in the axial zone of oceanic rifts: in these works, faulting has been interpreted as related to dike emplacement (Pollard et al., 1983; Curewitz and Karson, 1998; Rubin and Pollard, 1988; Stein et al., 1991), to the bending of the lithosphere (Tamsett, 1986), or as the consequence of a critical growth of extension fractures (Gudmundsson and Backstrom 1991; Forslund and Gudmundsson, 1992; Gudmundsson, 1992). Less is known on the development of normal faults on narrow continental rifts, where faulting has been mainly proposed to be due to the

* Corresponding author. Tel.: +39-06-54888027; fax: +39-06-54888201.
E-mail address: acocella@uniroma3.it (V. Acocella).

0191-8141/03/$ - see front matter © 2002 Elsevier Science Ltd. All rights reserved.
PII: S0191-8141(02)00047-0

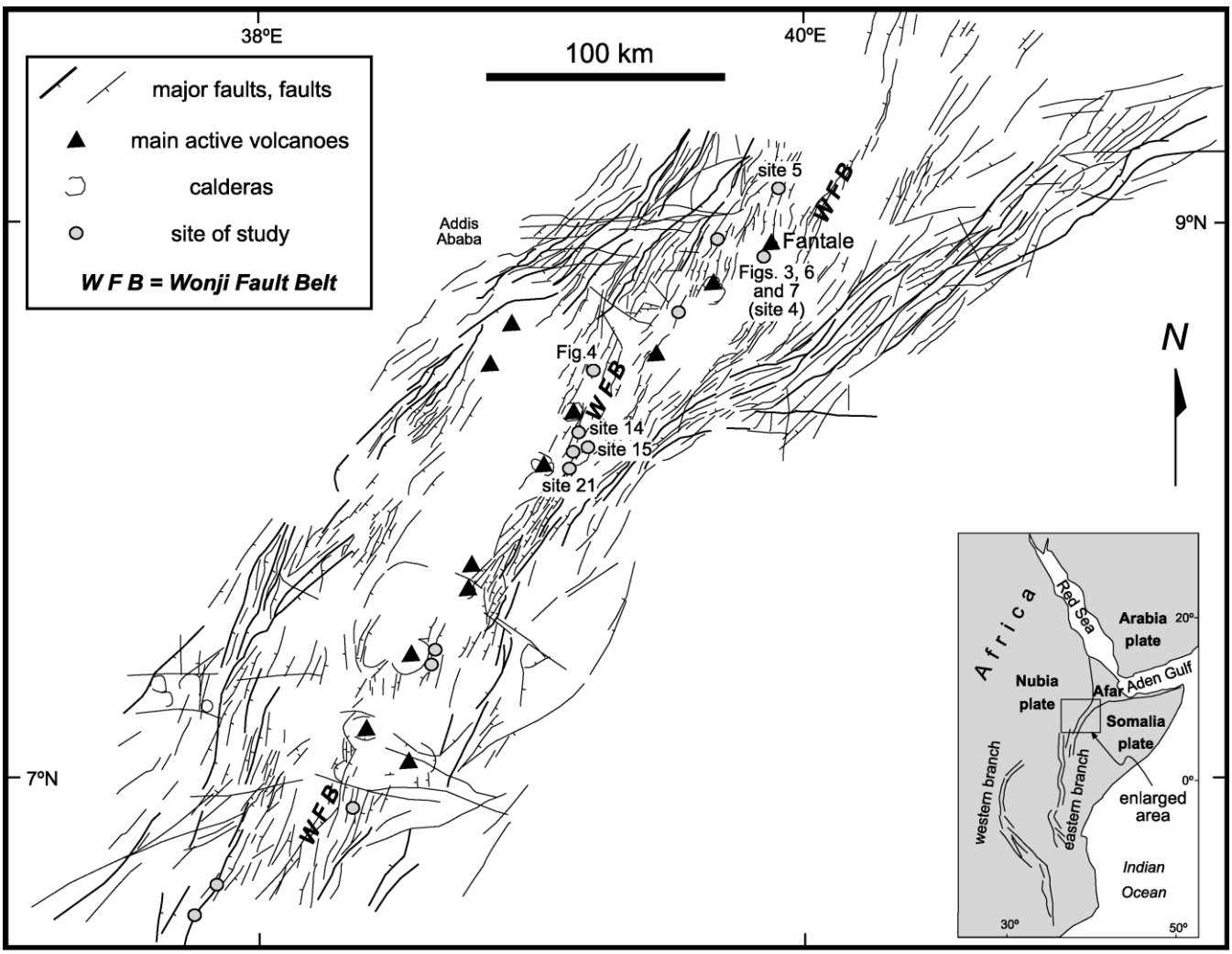

Fig. 1. Structural map of the Ethiopian Rift, interpreted from Landsat images. The inset shows a structural sketch of the East African Rift System; the Ethiopian Rift and its relationships with the Afar triple junction are shown.

reactivation of deeper pre-existing discontinuities (Smith and Mosley, 1993; Le Gall et al., 2000); in such a framework, the depth of fault nucleation is still debated (Cowie, 1998, and references therein).

This study thus aims at: (1) providing additional insights on the mechanism of formation and growth of normal faults in continental narrow rifts; (2) testing whether any of the proposed models of fault formation in oceanic rifts may be applied. For this purpose, we considered the axial zone of the Ethiopian part of the East African Rift System, where we performed field survey and fracture measurements. In particular, we focused on the geometry and kinematics of the normal faults and the relationships between normal faults and the nearby extension fractures. The collected data suggest that normal faults nucleate from extension fractures, once these reach a critical dimension, similarly to what has been proposed for the normal faults along the oceanic ridge of Iceland.

2. Tectonic framework

The East African Rift System is an Upper Tertiary–Quaternary intracontinental narrow rift, divided into an eastern and a western branch and composed of several interacting segments, from Mozambique to Afar (Fig. 1, inset; McConnell, 1972). At Afar, the East African Rift System forms a triple junction with the Gulf of Aden and Red Sea rifts, both characterized by a more advanced extensional stage (McKenzie et al., 1970; Le Pichon and Francheteau, 1978).

The Ethiopian Rift constitutes the northernmost part of the East African Rift System, connecting this with the Afar triple junction (Fig. 1, inset). The Ethiopian Rift started to develop during Miocene (Davidson and Rex, 1980; Woldegabriel et al., 1990), following a broad doming centered on the present Afar depression (Ebinger et al., 1989). During Pliocene and Quaternary, the Rift progressively deepened, evolving through a sequence of interacting

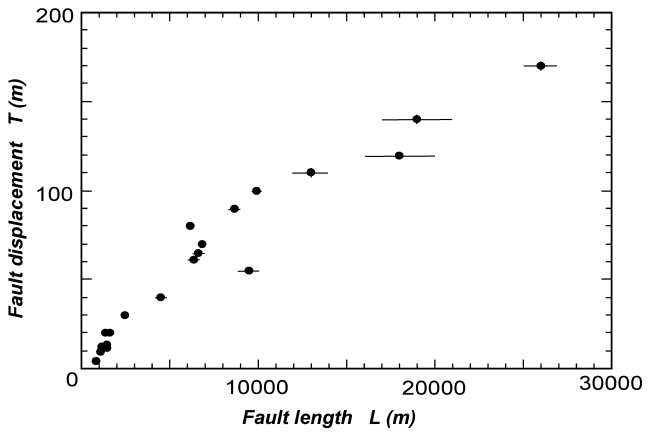

Fig. 2. The normal faults in the axial zone of the Ethiopian Rift show a proportion between their length L and their throw T.

half-graben segments (Hayward and Ebinger, 1996, and references therein). Widespread basaltic and rhyolitic volcanic activity was commonly associated with rifting (Woldegabriel et al., 1990; Chernet et al., 1998).

The youngest part of the Rift is the axial zone, which presently coincides with the Wonji Fault Belt, mainly formed during Quaternary (Fig. 1; Mohr, 1967, 1987). The Wonji Fault Belt is characterized by NNE–SSW-trending active extension fractures and normal faults, which in many places are associated with fissural or central volcanic activity (Gibson, 1969; Mohr, 1987; Chorowicz et al., 1994; Korme et al., 1997). The normal faults are in most cases arranged in a right stepping en-échelon configuration (Mohr, 1968; Boccaletti et al., 1998) and the vertical throws are in the order of several tens of meters (in the axial zone; Gibson, 1969) to several hundreds of meters (in the rift margins; Woldegabriel et al., 1990; Hayward and Ebinger, 1996).

3. Results

A field analysis was carried out in the axial part of the Ethiopian Rift, characterized by extension fractures and normal faults. Field analysis consisted of a detailed mapping and measuring of the geometry (length, strike, dip) and kinematics (dilation, throw, hanging wall tilt) of the normal faults. Most of the analysis was focused on Quaternary fractures. The Quaternary age of the fractures can be inferred by: (1) the age of the outcropping rocks (mostly consisting of Upper Pliocene–Quaternary basaltic lavas and welded ignimbrites; Davidson and Rex, 1980; Woldegabriel et al., 1990; Chernet et al., 1998; Tadewos et al., 1998); (2) the lack of significant erosion along most of the faults, as shown by the sharp asperities along their walls.

The active normal faults observed in the axial zone of the rift show proportional relationships between their length and throw (Fig. 2). Larger displacements are associated with longer faults, indicating interdependence between the horizontal and vertical dimensions of the faults; this is a result of the fact that the lengths (strike dimensions) of faults scale with their heights (dip dimensions) (Gudmundsson, 2000). Similar results were obtained in several extensional settings, both on oceanic and continental lithosphere (Cowie, 1998, and references therein).

All the observed Quaternary normal faults responsible for regional extension in the axial zone of the Ethiopian Rift, with throws larger than a meter, show an opening; these structures we call open normal faults (Fig. 3). The open fault is bordered by vertical walls, suggesting a subvertical geometry for the normal fault at the surface (Fig. 3). The layers in the hanging wall regularly show a tilt, usually between 10° and 50°, towards the downthrown side. Such a tilt is responsible for a real throw much larger than the apparent one observed at the sides of the open area.

Subvertical open normal faults are thus regularly found along the axial zone of the Ethiopian Rift, from north of the Fantale volcano (southern tip of the Afar depression; approx. N9°00′ Lat.) to Lake Abaya (approx. N6°30′ Lat.). In the axial zone of the rift, open faults have also been found along exposed sections of eroded fault scarps. Fig. 4 shows an example of an eroded fault scarp: the opening between the foot wall and the hanging wall has been filled by debris deposits. Open normal faults with a very similar geometry have been described along the oceanic ridge of Iceland (Gudmundsson, 1987a,b, 1992; Angelier et al., 1997).

The openings of the normal faults in the axial zone of the Ethiopian Rift tend to be proportional to the throw of the faults, either along the same fault or in different faults (Fig. 5). This indicates interdependence between the size of the fault and the amount of horizontal extension it accommodates. An example is shown in Fig. 6, which reports a representative case of open fault south of the Fantale volcano, in the axial part of the Ethiopian Rift.

A further feature of the normal faults in the axial part of the rift is their common association with subvertical extension fractures. No significant development of minor extension fractures subparallel to the normal faults was found along the foot wall and the hanging wall of the normal faults. Nevertheless, as for the example shown in Fig. 6, extension fractures often branch from the normal fault or replace limited parts of it, such as some inner portions and the tips. In particular, the throw of the active normal faults regularly decreases at the tips and the fault terminates as a subvertical extension fracture (Fig. 7), which progressively decreases in its opening along the strike of the fracture. Close similarities exist with the tips of the normal faults along the oceanic ridge of Iceland (Gudmundsson, 1992, and references therein).

The opening component (W; dashed line) and the shear component (throw T; solid line) of the tips of several normal faults are shown in Fig. 8. The tips of a normal fault are here defined as the extremities of the fault characterized by the progressive increase in the vertical displacement, until the maximum displacement is reached. The diagrams in Fig. 8

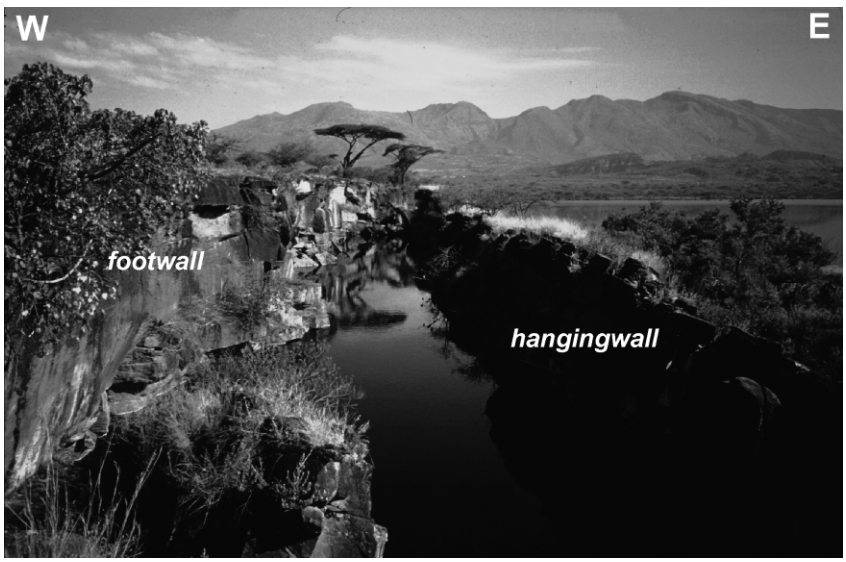

Fig. 3. Section of an active open normal fault in welded ignimbrites south of Fantale volcano, in the axial part of the Ethiopian Rift. The footwall and the hanging wall are separated by an open area. The exact location of the picture is shown in Fig. 6.

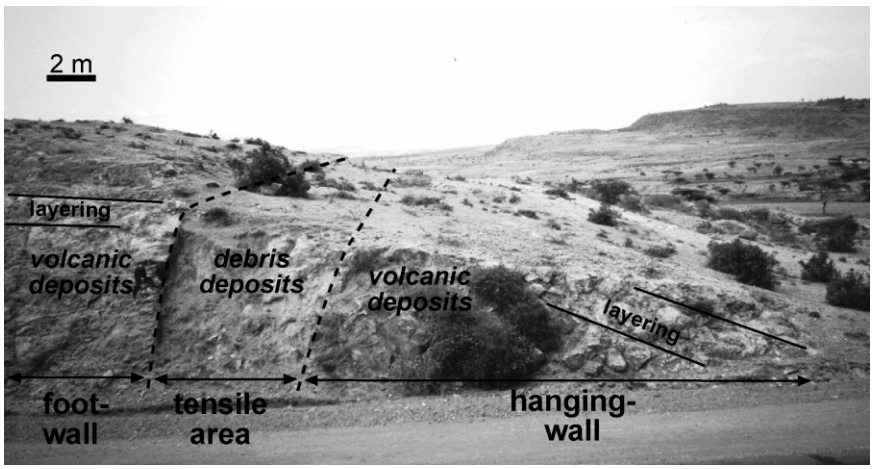

Fig. 4. Section of an open normal fault in the axial part of the Rift. The fault scarp is partly eroded and the open area between the footwall and the hanging wall is filled by debris deposits. Even though this fault is more mature than the one shown in Fig. 3, the two structures are identical.

show how the considered normal faults start, at the tips, as extension fractures and progressively increase their opening (dashed line); the vertical displacement (solid line) starts at an innermost position and then progressively increases (Fig. 8). Similar features were observed at the tips of normal faults in Iceland (Gudmundsson, 1987a,b) and in Utah (Cartwright and Mansfield, 1998).

Thus, these collected data show that: (1) there is a regular association between the throw and the dilational component of the normal faults in the axial zone of the Rift (Figs. 3–5); (2) the throw along the fault is proportional to its dilation (Fig. 5); (3) parts of the normal faults are pure extension fractures (this happens regularly at their tips; Figs. 6–8); (4) both the normal faults and the extension fractures are subvertical at surface (Figs. 3, 4 and 7). These observations suggest a genetic relation between the normal faults and the extension fractures in the axial zone of the rift.

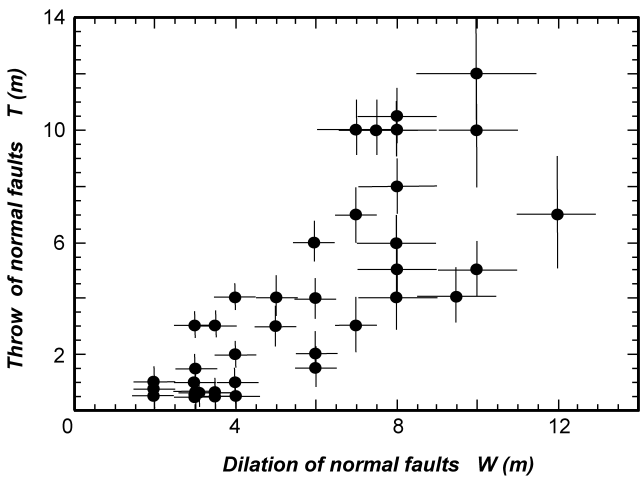

Fig. 5. The normal faults in the axial zone of the Ethiopian Rift show a proportion between their opening W and their throw T.

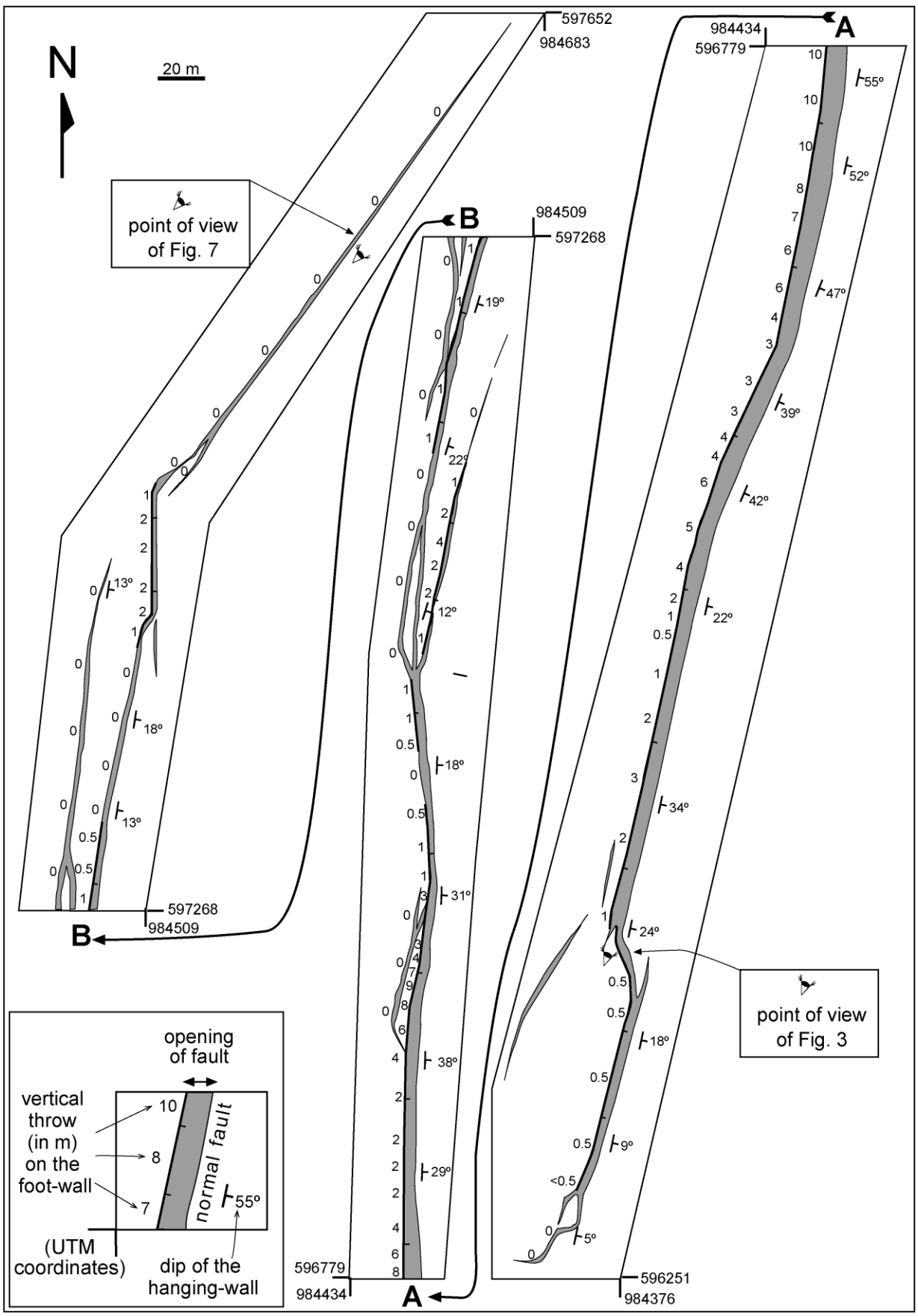

Fig. 6. Sketch map of a representative example of active open normal fault observed in welded ignimbrites south of Fantale volcano, in the axial part of the Ethiopian Rift. The numbers on the foot wall indicate the vertical displacement (in meters).

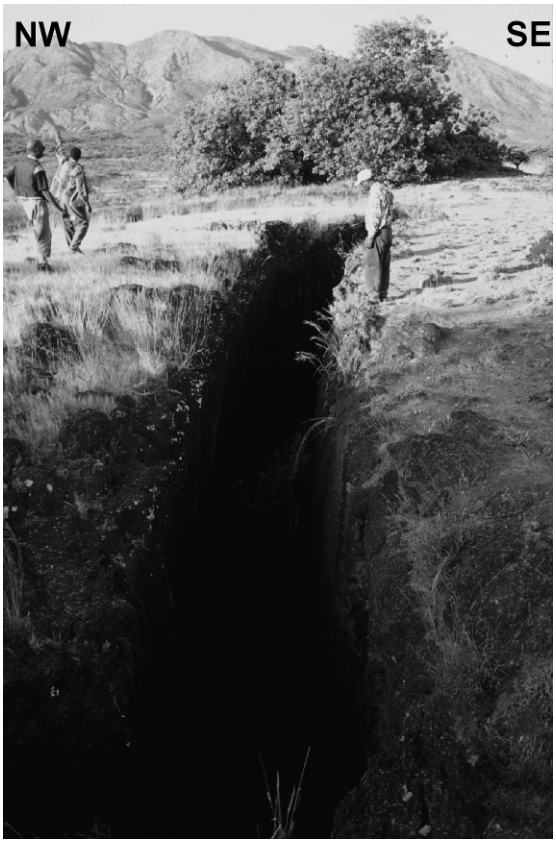

Fig. 7. Vertical extension fracture at the northern termination of the normal fault shown in Fig. 6.

The diagrams in Figs. 9 and 10 show the geometric relationships between the normal faults and the extension fractures in the axial zone of the Ethiopian Rift. Most of the extension fractures are less than 100–150 m long and no extension fractures longer than 400 m have been found (Fig. 9). In contrast, normal faults shorter than 800 m have not been observed and the mean length of the normal faults is several thousand meters (Fig. 9).

The measured dilation of the normal faults and extension fractures is shown in Fig. 10: the mean dilation of the extension fractures is around 2 m; extension fractures with an opening larger than 4 m have not been observed. The mean dilation of the normal faults (at least those shorter than 3000 m; see Fig. 9) is around 7 m, with a minimum value of 2 m. Thus, the mean dilation of the normal faults and the extension fractures shows a different distribution: even though a partial overlapping (between 2 and 4 m) occurs between the two distributions, the mean dilation of the extension fractures is several meters smaller than that shown by the normal faults (Fig. 10).

Based on the maximum dilation of the observed extension fractures $W \sim 4$ m and the longest fractures $L \sim 400$ m, the mean aspect ratio A (length/dilation) of the largest extension fractures is $A \sim 100$. Similar aspect ratios were measured for the extension fractures along the oceanic ridge of Iceland (Gudmundsson, 2000).

4. Discussion

Based on these considerations, we propose a mechanical model for the development of the normal faults from extension fractures, once these reach critical dimensions (Fig. 11). Before the onset of fracturing, a point A at surface is subject to a vertical stress (which is the resultant of lithostatic and tectonic stresses) $\sigma 1 = 0$ and a horizontal component (due to the tectonic stress) $\sigma 3 > -t$ (in the tensile regime), where t is the tensile strength (i.e. cohesion) of the rock. These conditions can be discussed in the underlying diagram, considering the Mohr–Coulomb criterion (Fig. 11a). Being the stress conditions mostly relevant on the left side of the diagram, these considerations are similar to those obtained with a Griffith failure criterion (see below).

By increasing the tectonic stresses, $\sigma 1$ at surface remains constant, whereas the horizontal component of stress $\sigma 3$ reaches the tensile strength of the rock; eventually, the stress at point A reaches the conditions for tensile failure (see related Mohr diagram) and the formation of an extension fracture at surface (Fig. 11b).

Once formed, the vertical fracture propagates along its strike and dip. During the propagation of the fracture at depth, the vertical stress at the tip A of the fracture becomes $\sigma 1 = \rho g h$, where ρ is the density of the rocks, g is the acceleration due to gravity and h is the depth; to ensure fracture propagation at depth, the horizontal (lithostatic plus tectonic) stress concentration at the tip of the fracture must remain $\sigma 3 = -t$ (Fig. 11c). However, at a critical depth h_c, the rock can no longer sustain the tensile stresses required to maintain a pure tensile behaviour. This occurs when the vertical component at the tip A of the fracture is $\sigma 1 = \rho g h_c = t$ (Fig. 11d); the horizontal component $\sigma 3$ remains constant and equal to the tensile strength at the tip A of the fracture (Fig. 11d). Considering, for our study, a mean tensile strength of the rocks $t = 6$ MPa (Jaeger and Cook, 1979; Gudmundsson, 1992, and references therein), a mean in situ density $\rho = 2400$ kg m^{-3} (Gudmundsson, 1988) and $g = 9.8$ m s^{-2}, such critical depth is:

$$h_c = t/\rho g \sim 260 \text{ m}. \quad (1)$$

Considering the Griffith criterion for fracture initiation, the critical depth is (Gudmundsson, 1992):

$$h_c = 3t/\rho g \sim 780 \text{ m}. \quad (2)$$

Thus, depending on the criterion (Mohr–Coulomb or Griffith) we use, the maximum depth for an extensional fracture is between ~260 and ~780 m. These values may increase if the presence of pore pressure in the rocks is taken into account.

As shown in the Mohr–Coulomb diagram in Fig. 11d and according to the criteria of brittle failure, when an extension fracture attains that critical depth, it becomes a fault (Forslund and Gudmundsson, 1992, and references therein). The normal faults start to form when they reach

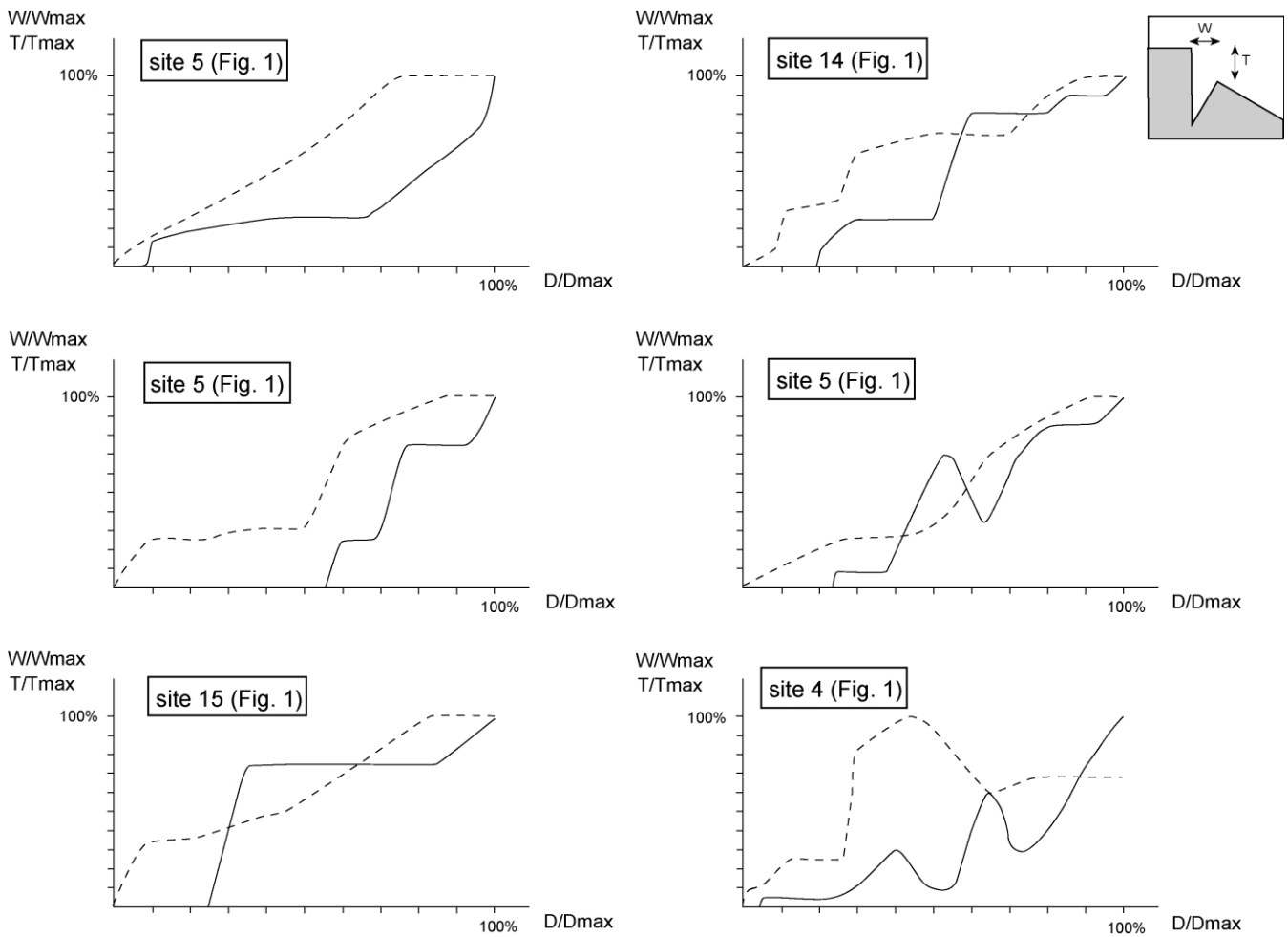

Fig. 8. Variation of the dilational (opening *W*, dashed lines) and shear (throw *T*, solid lines) components from the tips of the normal faults (where the throw is zero) to the central portion of the fault (where the maximum displacement is reached). See text for further details.

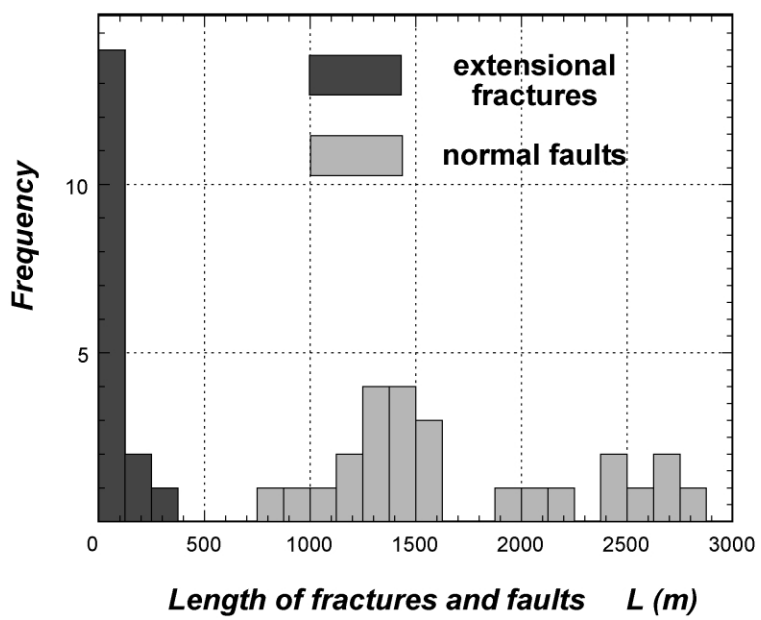

Fig. 9. Distribution of the length (*L*) of normal faults and extension fractures observed along the axial part of the Rift. The horizontal scale has an upper limit at 3000 m.

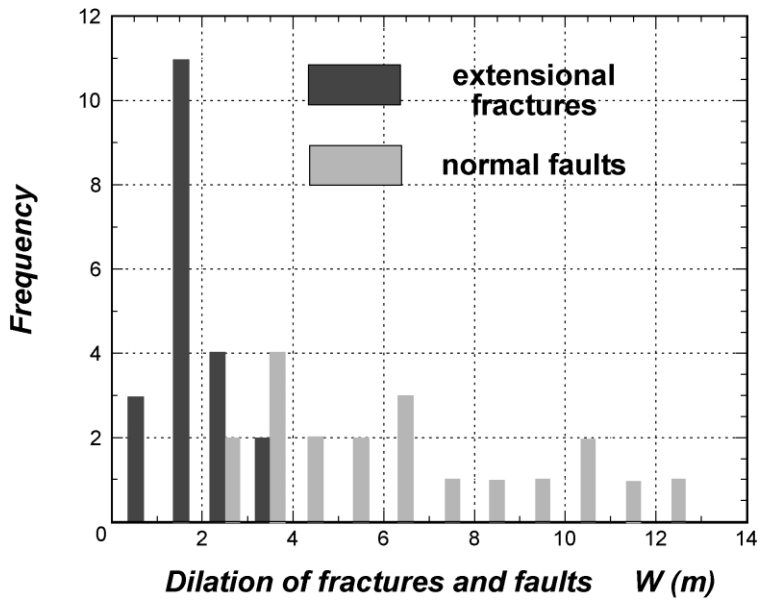

Fig. 10. Distribution of the opening (W) of normal faults and extension fractures observed along the axial part of the Rift.

definite measures at surface, characterized by a dilation W between 2 and 4 m and a length $L \sim 800$ m (Figs. 9 and 10). Normal faults in various settings have an aspect ratio (strike dimension/dip dimension) >1 (Nicol et al., 1996, and references therein); thus, the minimum length (800 m) of the faults observed in Ethiopia is more consistent with the critical (minimum) depth h_c calculated in Eq. (1) than the one calculated in Eq. (2).

Once the fault has formed, it grows further, propagating both downward and along strike. Both the vertical stress $\sigma 1$ and the horizontal stress $\sigma 3$ at the tip A exceed the tensile strength of the rock (Fig. 11e). As shown in the Mohr–Coulomb diagram in Fig. 11e, the stress conditions at the tip A of the normal fault are now constantly characterized by shear failure. The fault at this stage is no longer vertical, as the shear failure conditions (as shown in the Mohr–Coulomb diagram) require that an angle α forms between the vertical principal stress and the fault plane at depth (Fig. 11e; Anderson, 1951). In such a framework, the synthetic tilt regularly observed in the hanging wall of the normal faults is interpreted to be the surface expression of the drag induced by the change of dip of the fault plane at depth. If such a change in the dip is abrupt and shallow (<1 km of depth, as in Fig. 11e), the higher friction in this part of the fault may form a synthetic tilt in the hanging wall at the surface, consistently with theoretical considerations

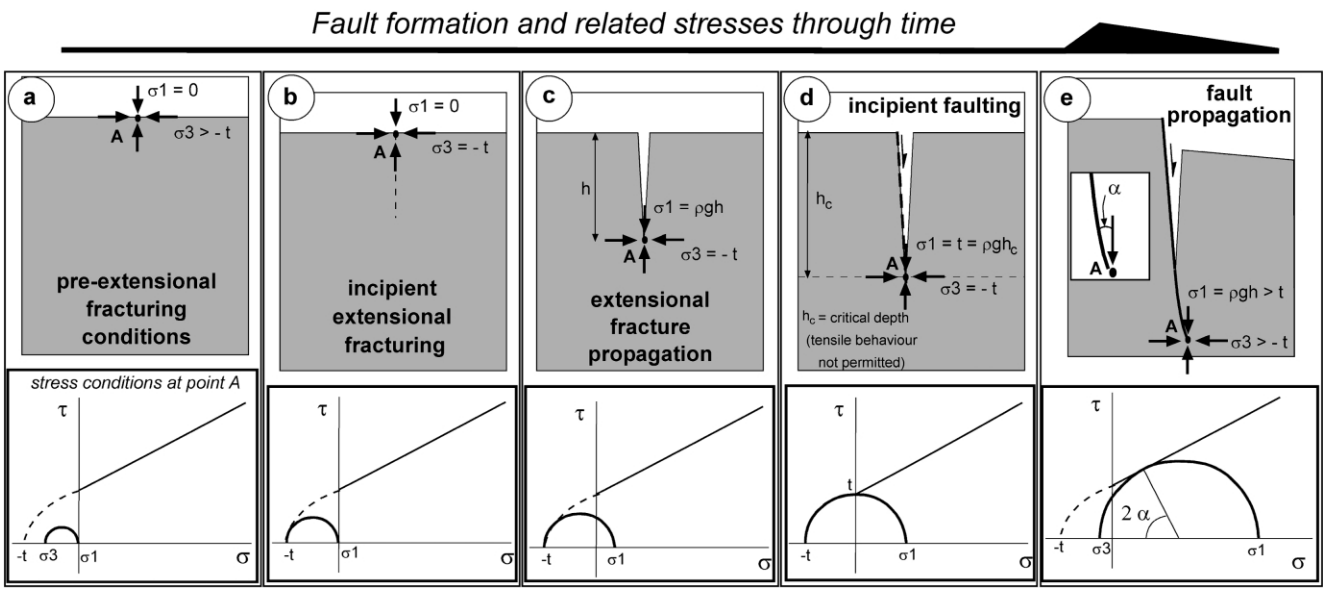

Fig. 11. Mechanical model proposed to explain the formation of normal faults from the progressive growth of the extension fractures in the axial part of the Ethiopian Rift. See text for further details.

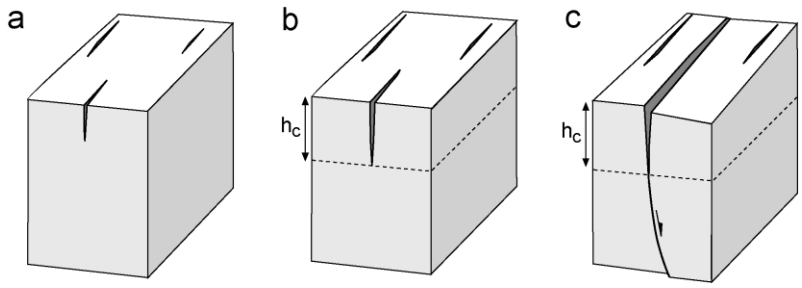

Fig. 12. Simplified model of formation and growth of the normal faults in the axial part of the Ethiopian Rift. Once the extension fractures form (stage a), they reach a critical depth h_c (stage b), turning into normal faults (stage c).

(Gudmundsson, 1992, and references therein). Conversely, a gentle change in the dip along listric faults becoming subhorizontal at depth usually generates an antithetic tilt in the hanging wall at the surface.

A schematic evolutionary model is proposed in Fig. 12. The growth of an extension fracture is characterized by its propagation downward and along strike (Fig. 12a). The fracture reaches a critical depth, below which the tensile stresses can no longer be sustained (in the absence of fluids) (Fig. 12b). As a consequence, it turns into a normal fault; the propagation of the fault at depth requires a progressive decrease in its dip (Fig. 12c).

An alternative model of formation of the normal faults may be proposed. According to this model, the observed downward narrowing extensional fractures may be the product of an outer-arc extension bending strain related to the upward propagation of a blind normal fault. In such a framework, the upward propagating normal fault may be responsible for a broad flexure (and thus tilting) at surface, which, in turn, induces extension in the outer portion and the formation of extensional fractures. Thus, outer arc extension fractures propagate downward, while the blind normal fault propagates upward from depth.

Even though a similar mechanism has been proposed for the formation of normal faults in the Kenya Rift (Le Gall et al., 2000), two observations do not support such a model in the Ethiopian Rift. (1) No tilt in the foot wall and no broad fracturing outside the fault (in the hanging wall and footwall) have been observed; this suggests the absence of a flexure related to blind faulting. (2) The pure dilational component at the tips of the faults, where $T = 0$ (Fig. 8) is usually not accompanied with a significant tilt of the hanging wall (as shown in Fig. 7) or footwall; this suggests that the dilational component is not related to the observed hanging wall tilt and thus the fracture cannot be the result of a flexure due to an uprising blind fault.

The observed normal faults in the axial part of the Ethiopian Rift have very close similarities with the normal faults observed along the oceanic ridge of Iceland (Gudmundsson, 1987a,b; Acocella et al., 2000). Both are subvertical open faults, terminate as extension fractures and show a hanging wall tilt towards the downthrown side. As a consequence, the mechanism of fault formation proposed here is similar to the one which has been proposed to explain faulting processes along oceanic ridges (Gudmundsson and Backstrom 1991; Forslund and Gudmundsson, 1992; Gudmundsson, 1992; Wright, 1998). These similarities suggest a common fracture mechanism and rifting process along diverging plates, independently from the oceanic or continental nature of the lithosphere.

5. Conclusions

The collected data in the axial zone of the Ethiopian Rift show that the normal faults are subvertical and open, with a dilation proportional to the throw, and terminate as extension fractures. The normal faults are longer and have a larger dilation than the extensional fractures. The data suggest that the normal faults nucleate from larger extension fractures. When the extension fractures reach a critical depth, between 300–700 m, the tensile stresses can no longer be sustained and a failure behavior controls the further propagation of the ruptures at depth. The similarities between the mechanism of faulting at oceanic rifts (such as Iceland) and continental rifts (such as Ethiopia) suggest common rifting processes along diverging plates, independently from the oceanic or continental nature of the lithosphere.

Acknowledgments

The Authors wish to thank R. Funiciello for encouragement. B. Abele partly participated to the field work. The reviewers D.A. Ferrill and A. Gudmundsson are kindly acknowledged for their useful suggestions. This work was financed with MURST funds (F. Salvini responsible).

References

Acocella, V., Gudmundsson, A., Funiciello, R., 2000. Interaction and linkage of extensional fractures: examples from the rift zone of Iceland. Journal of Structural Geology 22, 1233–1246.

Anderson, E.M., 1951. The Dynamics of Faulting, Oliver and Boyd, Edinburgh, 206pp.

Angelier, J., Bergerat, F., Dauteuil, O., Villemin, T., 1997. Effective tension–shear relationships in extensional fissure swarms, axial rift zone of northeastern Iceland. Journal of Structural Geology 19, 673–685.

Boccaletti, M., Bonini, M., Mazzuoli, R., Abebe, B., Piccardi, L., Tortrici, L., 1998. Quaternary oblique extensional tectonics in the Ethiopian Rift (Horn of Africa). Tectonophysics 287, 97–116.

Bonatti, E., 1985. Punctiform initiation of seafloor spreading in the Red Sea during transition from a continental to an oceanic rift. Nature 316, 33–37.

Bosworth, W., 1985. Geometry of propagating continental rifts. Nature 316, 625–627.

Buck, W.R., 1991. Modes of continental lithospheric extension. Journal of Geophysical Research 96, 20161–20178.

Cartwright, J.A., Mansfield, C.S., 1998. Lateral displacement variation and lateral tip geometry of normal faults in the Canyonlands National Park, Utah. Journal of Structural Geology 20, 3–19.

Chernet, T., Hart, W., Aronson, J.L., Walter, R.C., 1998. New age constraints on the timing of volcanism and tectonism in the northern Main Ethiopian Rift–southern Afar transition zone (Ethiopia). Journal of Volcanology and Geothermal Research 80, 267–280.

Chorowicz, J., Collet, B., Bonavia, F.F., Korme, T., 1994. Northwest to north-northwest extension direction in the Ethiopian Rift deduced from the orientation of extension structures and fault-slip analysis. Geological Society of America Bulletin 105, 1560–1570.

Cowie, P.A., 1998. Normal fault growth in three-dimensions in continental and oceanic crust. In: Buck, W.R., Delaney, P.T., Karson, J.A., Lagabrielle Y. (Eds.), Faulting and Magmatism at Mid-Ocean Ridges, Geophysical Monograph 106, pp. 325–348.

Curewitz, D., Karson, J.A., 1998. Geological consequences of dike intrusion at mid-ocean ridge spreading centres. In: Buck, W.R., Delaney, P.T., Karson, J.A., Lagabrielle Y. (Eds.), Faulting and Magmatism at Mid-Ocean Ridges, Geophysical Monograph 106, pp. 117–136.

Davidson, A., Rex, D.C., 1980. Age of volcanism and rifting in southwestern Ethiopia. Nature 283, 657–658.

Ebinger, C.J., 1989. Tectonic development of the western branch of the East African rift system. Geological Society of America Bulletin 101, 885–903.

Ebinger, C.J., Crow, M.J., Rosendahl, B.R., Livingstone, D.A., LeFournier, J., 1984. Structural evolution of Lake Malawi, Africa. Nature 308, 627–629.

Ebinger, C.J., Rosendahl, B.R., Reynolds, D.J., 1987. Tectonic model of the Malawi rift, Africa. Tectonophysics 141, 215–235.

Ebinger, C.J., Bechtel, T.D., Forsyth, D.W., Bowin, C.O., 1989. Effective elastic plate thickness beneath the East African and Afar plateaus and dynamic compensation of the uplifts. Journal of Geophysical Research 94, 2883–2901.

Forslund, T., Gudmundsson, A., 1991. Crustal spreading due to dikes and faults in southwest Iceland. Journal of Structural Geology 13, 443–457.

Forslund, T., Gudmundsson, A., 1992. Structure of Tertiary and Pleistocene normal faults in Iceland. Tectonics 11, 57–68.

Gibson, I., 1969. The structure and volcanic geology of an axial portion of the Main Ethiopian Rift. Tectonophysics 8, 561–565.

Gudmundsson, A., 1987a. Geometry, formation and development of tectonic fractures on the Reykjanes Peninsula, southwest Iceland. Tectonophysics 139, 295–308.

Gudmundsson, A., 1987b. Tectonics of the Thingvellir fissure swarm, Iceland. Journal of Structural Geology 9, 61–69.

Gudmundsson, A., 1988. Effect of tensile stress concentration around magma chambers on intrusion and extrusion frequencies. Journal of Volcanology and Geothermal Research 35, 179–194.

Gudmundsson, A., 1992. Formation and growth of normal faults at the divergent plate boundary in Iceland. Terra Nova 4, 464–471.

Gudmundsson, A., 1995. Infrastructure and mechanics of volcanic systems in Iceland. Journal of Volcanology and Geothermal Research 64, 1–22.

Gudmundsson, A., 2000. Fracture dimensions, displacements and fluid transport. Journal of Structural Geology 22, 1221–1231.

Gudmundsson, A., Backstrom, K., 1991. Structure and development of the Sveinagja graben, northeast Iceland. Tectonophysics 200, 111–125.

Hayward, N.J., Ebinger, C.J., 1996. Variations in the along-axis segmentation of the Afar Rift system. Tectonics 15, 244–257.

Jaeger, J.C., Cook, N.G., 1979. Fundamentals of Rock Mechanics, Chapman and Hall, London, 515pp.

Kazmin, V.G., Byakov, A.F., 2000. Magmatism and crustal accretion in continental rifts. Journal of African Earth Sciences 30, 555–568.

Korme, T., Chorowicz, J., Collet, B., Bonavia, F.F., 1997. Volcanic vents rooted on extension fractures and their geodynamic implications in the Ethiopian Rift. Journal of Volcanology and Geothermal Research 79, 205–222.

Le Gall, B., Tiercelin, J.J., Richert, J.P., Gente, P., Sturchio, N.C., Stead, D., Le Turdu, C., 2000. A morphotectonic study of an extensional fault zone in a magma-rich rift: the Baringo Trachyte Fault System, central Kenya Rift. Tectonophysics 320, 87–106.

Le Pichon, X., Francheteau, J., 1978. A plate tectonic analysis of the Red Sea–Gulf of Aden area. Tectonophysics 46, 369–406.

Martinez, F., Cochran, J.R., 1988. Structure and tectonics of the northern Red Sea: catching a continental margin between rifting and drifting. Tectonophysics 150, 1–32.

McConnell, R.B., 1972. Geological development of the Rift System of Eastern Africa. Geological Society of America Bulletin 83, 2549–2572.

McKenzie, D.P., Davies, D., Molnar, P., 1970. Plate tectonics of the Red Sea and East Africa. Nature 226, 243–248.

Mohr, P., 1967. Major volcano–tectonic lineament in the Ethiopian Rift System. Nature 213, 664–665.

Mohr, P., 1968. Transcurrent faulting in the Ethiopian Rift System. Nature 218, 938–941.

Mohr, P., 1987. Patterns of faulting in the Ethiopian Rift Valley. Tectonophysics 143, 169–179.

Morley, C.K., 1988. Variable extension in Lake Tanganyika. Tectonics 7, 785–801.

Needham, H.D., Choukroune, P., Cheminee, J.L., Le Pichon, X., Francheteau, J., Tapponier, P., 1976. The accreting plate boundary: Ardoukoba Rift (northeast Africa) and the oceanic rift valley. Earth and Planetary Science Letters 28, 439–453.

Nelson, R.A., Patton, T.L., Morley, C.K., 1992. Rift-segment interaction and its relation to hydrocarbon exploration in continental rift systems. American Association Petroleum Geology Bulletin 76, 1153–1169.

Nicol, A., Watterson, J., Walsh, J.J., Childs, C., 1996. The shapes, major axis orientation and displacement patterns of fault surfaces. Journal of Structural Geology 18, 235–248.

Pollard, D.D., Delaney, P.T., Duffield, W.A., Endo, E.T., Okamura, T., 1983. Surface deformation in volcanic rift zones. Tectonophysics 94, 541–584.

Rosendahl, B.R., 1987. Architecture of continental rifts with special reference to East Africa. Annual Review Earth Planetary Sciences 15, 445–503.

Rubin, A.M., Pollard, D.D., 1988. Dike-induced faulting in rift zones of Iceland and Afar. Geology 16, 413–417.

Scholz, C.H., Contreras, J.C., 1998. Mechanics of continental rift architecture. Geology 26, 967–970.

Smith, M., Mosley, P., 1993. Crustal heterogeneity and basement influence on the development of the Kenya Rift, East Africa. Tectonics 12, 591–606.

Stein, R.S., Briole, P., Ruegg, J.C., Tapponier, P., Gasse, F., 1991. Contemporary, Holocene and Quaternary deformation of the Asal Rift, Djibuti: implications for the mechanics of slow spreading ridges. Journal of Geophysical Research 96, 21789–21806.

Tadewos, C., Hart, W.K., Aronson, J.L., Walter, R.C., 1998. New age constraints on the timing of the volcanism and tectonism in the northern

Main Ethiopian Rift–Southern Afar transition zone (Ethiopia). Journal of Volcanology and Geothermal Research 80, 267–280.

Tamsett, D., 1986. Median Valley tectonics: air photographs of the Ghoubbet–Asal Rift, Afar. Tectonophysics 131, 75–87.

Woldegabriel, G., Aronson, J.L., Walter, R.C., 1990. Geology, geochronology and rift basin development in the central sector of the Main Ethiopian Rift. Geological Society of America Bulletin 102, 439–458.

Wright, D.J., 1998. Formation and development of fissures at the East Pacific Rise: implications for faulting and magmatism at Mid-Ocean Ridges. In: Buck, W.R., Delaney, P.T., Karson, J.A., Lagabrielle Y. (Eds.), Faulting and Magmatism at Mid-Ocean Ridges, Geophysical Monograph 106, pp. 137–151.